Auto-catalytic high-performance recyclable carbon fiber reinforced epoxy composites mediated by neighboring group participation

Zihan Zhao, Jianqiao Wu, Liang Gao, Haojie Gong, Zhongkai Guo, Baoyan Zhang, Min-Hui Li, Jun Hu

Auto-catalytic high-performance recyclable carbon fiber reinforced epoxy composites mediated by neighboring group participation

Zihan Zhao,[a] Jianqiao Wu,[a,b] Liang Gao,[c] Haojie Gong,[a] Zhongkai Guo,[a] Baoyan Zhang,[c] Min-Hui Li[a,d] and Jun Hu[*a]

[a]Beijing Advanced Innovation Center for Soft Matter Science and Engineering, Beijing University of Chemical Technology, Beijing 100029, China

[b]College of Materials and Chemical Engineering, Chuzhou University, West Huifeng Road 1, Langya District, Chuzhou 239000, China

[c]Department of Resin & Prepreg, AVIC Manufacturing Technology Institute Composite Technology Center, Shijun Road 1, Shunyi District, Beijing 101300, China

[d]Chimie ParisTech, PSL University, CNRS, Institut de Recherche de chimie, Paris 75005, France

*Corresponding authors

Email: jhu@mail.buct.edu.cn (Jun Hu)

Abstract

Epoxy-based carbon fiber reinforced composites (CFRCs) are leading contenders in high-tech fields. However, the majority of CFRCs consisted of thermoset matrix and carbon fibers (CFs) are costly to produce and difficult to recycle. In this study, this problem has been solved by a simple strategy to prepare high-performance recyclable CFRCs from commercial-scale low-cost phthalic anhydride (PA) and diglycidyl ester of aliphatic cyclo (DGEAC). The rigid DGEAC/PA networks resulted in a glass transition temperature of ~214°C, a tensile strength of ~79 MPa, and a Young's modulus of ~1.84 GPa. More importantly, the neighboring group participation (NGP) effect facilitated the transesterification reactions (TERs), making DGEAC/PA networks degradable in ethylene glycol. Accordingly, the CF/DGEAC/PA composites exhibited good mechanical properties comparable to conventional epoxy CFRCs, and the CFs could be recycled completely with similar features of the virgin CFs. This work provides an auto-catalytic sustainable approach for high-performance degradable CFRCs.

Keywords: (A) Polymer-matrix composites (PMCs); (A) Thermosetting resin; (A) Recycling; (D) Microstructural analysis.

1. Introduction

Epoxy-based carbon fiber reinforced composites (CFRCs) own superior combination of high strength-to-weight ratio, good chemical resistance and dimensional stability, which have been leading contenders in high-tech fields like aerospace, military manufacturing, and automotive industries [1]. Nevertheless, the intrinsic permanent cross-linked structures of epoxy matrix make CFRCs difficult to be recycled once they are damaged or at the end of the service life, causing serious economic and environmental burdens [2]. At present, the most frequently used recycling technologies of CFRPs are mechanical recycling and thermochemical recycling [3,4]. The mechanical recycling method normally involves the grinding of waste composites and the reuse of resulting scrap pieces as filler in new composites or energy combustion [5]. But the commercial value of this method is quite low because the strength of virgin carbon fibers (CFs) is not recovered. While for thermochemical cycling, although the loss in tensile strength of the recycled CFs is negligible, supercritical chemicals and high energy consumption are often required during the recycling process, which are hazardous and economically unfavorable in large scale production [6,7]. All these issues in recycling CFRPs are in direct conflict with the concept of sustainable development in modern society. Therefore, it still remains a challenge to fabricate high performance epoxy-based CFRCs with green recyclable ability at low cost.

The introduction of dynamic covalent bonds into the cross-linked thermosets matrix endows CFRCs with degradable and recyclable properties. So far, the dynamic covalent bonds used in CFRCs mainly include acetal bonds [8], imine bonds [9-11], ester bonds [12-14] and bisulfide bonds [15,16]. For example, Zhu and co-workers [9] prepared an imine

bond-tailored biobased epoxy resin by using the epoxy monomer of vanillin and diamines as raw materials, which exhibited high glass transition temperature (T_g) of 172°C and good mechanical property with a tensile strength of 81 MPa. Under acidic condition, this epoxy resin completely degraded at room temperature, consequently making the corresponding CFRCs achieve a rapid recovery of CFs. While the lack of acid-resistance and stability of imine bond also limited their actual productions. Compared with imine bonds, ester bonds have superior thermal and chemical stability, and is one of the most frequently used dynamic covalent bonds. Qi group [12] reported an epoxy-based CFRCs containing dynamic ester bonds by using epoxy resin/fatty acid matrix developed by Leibler [17]. Benefiting from the transesterification reactions (TERs) catalyzed by zinc acetate, the valuable CFs have been recovered completely with a recovery efficiency close to 100%. However, the extrinsic catalysts added to promote the occurrence of TERs also raise the cost and weaken the performance of CFRCs because of their poor compatibility with the substrate. Therefore, a conflict exists between the high performance and the occurrence of TERs promoted by extrinsic catalyst [18]. To resolve this issue, some alternative strategies have been proposed in recent years. Zhang and co-workers [19,20] found that the presence of a large amount of accessible hydroxyl groups in epoxy resin played a role like catalysts to accelerate the TERs. Meanwhile, Du. Prez [21] introduced the concept of neighboring group participation (NGP) to produce an auto-catalytic polyester by using diphthalic anhydride and polyol. During the TERs process, the neighboring groups that covalently combined with the reaction center in the network preferred to form a ring transition state, which spontaneously promoted the reactivity of TERs without any extrinsic regulation. Apparently, these auto-catalytic

strategies make the simultaneous realization of the high performance and the occurrence of TERs possible [22-24].

Inspired by these auto-catalytic works, as well as the demands of high-performance CFRCs with green recyclable ability, herein, in this research we designed and synthesized an auto-catalytic high-performance recyclable epoxy-based CFRCs by using phthalic anhydride (PA) and diglycidyl ester of aliphatic cyclo (DGEAC) as matrix while carbon fiber T300 as reinforcement (Scheme 1). In this network, both PA and DGEAC are commercial-scale reagents at low price, and their rigid backbones make the cross-linked networks own good thermal and mechanical performance. More importantly, the generated free carboxylic acid on *o*-position of benzene rings after curing can accelerate the TERs as an intrinsic catalyst via neighboring group participation (NGP), avoiding the adverse effects of extrinsic catalysts and endowing the CFRCs with recyclability. The results showed that the cured DGEAC/PA had superior mechanical and thermal properties (T_g of 165-214°C, T_d of 232-316°C, tensile strength of 68-79 MPa, modulus of 1.71-1.84 GPa), as well as good solvent resistance. Promoted by the NGP effect, the DGEAC/PA completely degraded in ethylene glycol (EG). Accordingly, the CF/DGEAC/PA composites by laminating DGEAC/PA with CFs exhibited the comparable mechanical properties with conventional epoxy composites. In addition, the CFs can be fully recovered in a non-destructive manner by soaking CF/DGEAC/PA in EG at 190°C, which was quite difficult for conventional epoxy CFRCs. In these epoxy CFRCs containing dynamic covalent bonds, the simultaneous realization of high performance comparable to commercial products, good resistance to common solvents, and low-cost recyclability without extrinsic catalysts were achieved for the first time. This work is in line with the requirement of sustainable development and carbon neutrality.

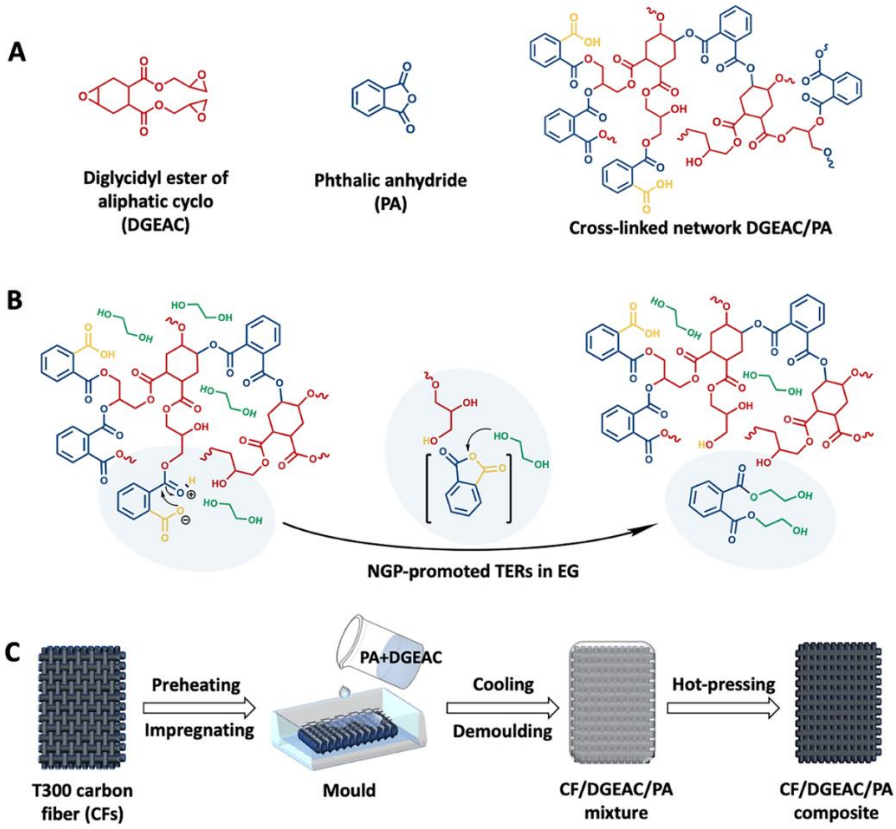

Scheme 1. (A) Chemical structures of the monomers and the cross-linked DGEAC/PA networks. (B) NGP-promoted transesterification (TERs) of DGEAC/PA networks in ethylene glycol (EG). (C) Schematic illustration of the preparation of CF/DGEAC/PA composites.

2. Experimental section

2.1 Materials

Diglycidyl ester of aliphatic cyclo (DGEAC, Tianjin Jindong Chem), phthalic anhydride (PA, Inno Chem), woven carbon fiber T300 (GW3011, Weihai Tuozhan), and ethylene glycol (EG, Inno Chem) were used as purchased without further purification.

2.2 Synthesis of DGEAC/PA networks

Initially, PA was mixed with DGEAC by a homogenizer in a beaker at 85°C, and the mixture was heated under a gradual increase of temperature to 130°C within 30 min, affording a prepolymer. Subsequently, the prepolymer was poured into a stainless mould with a dimension of 100 mm × 80 mm × 1 mm at 130°C and placed in a press vulcaniser. After curing at 130°C for 1 h, 150°C for 2 h, and 180°C for 1 h at a pressure of 10 tons, the DGEAC/PA networks was obtained with different stoichiometric ratios (R = 0.7, 0.85, and 1.0, anhydride/epoxy group).

2.3 Preparation of CF/DGEAC/PA composites

PA was firstly added into DGEAC in a beaker at 85°C and heated up gradually in constant agitation until a homogeneous prepolymer of DGEAC/PA (R = 0.7) formed. Next, five slices of woven CFs (T300) were impregnated with the prepolymer. After cooling to room temperature, the mixture of CF/DGEAC/PA was demoulded and cured in a hot press at 130°C for 1 h, 150°C for 2 h, and 180°C for 1 h at a pressure of 10 tons.

2.4 Degradation of DGEAC/PA networks

In general, the sample of DGEAC/PA (~30 mg) with a dimension of 5 mm × 2 mm × 1 mm was placed in a vial containing 10 mL ethylene glycol (EG), and then moved to an oven at the test temperature (190°C, 195°C, and 200°C) under atmospheric pressure. After different degradation time, the sample was taken out of the vial. The surface solvent of the sample was removed with a filter paper, and the sample was dried in an oven at 190°C for 10 h. After that, the weight of the residual sample was recorded for studying the degradation kinetics. Each experiment was repeated for at least three times. In addition, the degradation products were analyzed by high-performance liquid chromatography-mass spectrometry (HPLC-MS).

2.5 Recycling of CF/DGEAC/PA composites

Initially, the sample of CF/DGEAC/PA composites (R = 0.7) with a dimension of 5 mm × 2 mm × 1 mm was immersed in 10 mL EG in a vial, and then moved to an oven at 190°C under atmospheric pressure. After different degradation time, the sample was taken out of the vial. The surface solvent of the sample was removed with a filter paper, and the sample was dried at 190°C for 10 h. In the end, the residual weight was recorded for studying the degradation kinetics. Each experiment was repeated for at least three times. For analyzing the degradation process in depth, the cleavage surface of samples after different degradation time were observed by scanning electronic microscopy (SEM).

2.6 Characterization

Gel content test: the gel content was measured by the immersion method. The sample (m_0, ~30 mg) was immersed in acetone for 20 h at room temperature. After that, the insoluble part was dried in a vacuum over at 80°C for 12 h and then weighted (m_1). The gel content of the sample was calculated according to the equation (eq 1):

$$\text{Gel content (\%)} = \frac{m_1}{m_0} \times 100\% \qquad \text{(eq 1)}$$

Swelling test: the swelling ratio was measured by immerging the sample (m_0, ~30 mg) in acetone at room temperature. When the absorption reached equilibrium, the sample was taken out of the solution, and the excessive solvent on surface was removed with the filter paper. The swollen sample was weighted (m_1), and the swelling ratio was calculated according to the equation (eq 2):

$$\text{Swelling ratio (\%)} = \frac{m_1 - m_0}{m_0} \times 100\% \qquad \text{(eq 2)}$$

Differential scanning calorimetry test (DSC): the curing method and the glass transition temperature (T_g) after curing were determined by a differential scanning calorimeter (TA-Q20). The samples (5 mg) were sealed in aluminum crucibles and then heated from 25 to 250°C at a heating rate of 5 °C/min.

Fourier transform infrared spectroscopy (FTIR): the determination of the changes in functional groups was conducted on a spectrophotometer (Nicolet iS5) by using KBr pellet method. All samples were scanned from 4000 to 500 cm^{-1}.

Thermal stability test (TGA): the thermal stability of DGEAC/PA networks was measured by using a thermogravimetric analyzer (TA-Q50). The samples (~5 mg) were loaded into alumina crucibles and heated from 30 to 800°C at a heating rate of 10 °C/min under nitrogen atmospheres.

Dynamic mechanical test: the dynamic mechanical properties of DGEAC/PA networks were measured by using dynamic mechanical analyzer (TA-Q850) under tensile mode. The sample with a dimension of 30 mm × 5 mm × 1 mm was scanned from 30 to 260°C at a heating rate of 5 °C/min. The amplitude was set at 10 μm and the frequency was 1 Hz.

Stress relaxation test: the stress relaxation was measured using DMA (TA-Q850). The sample DGEAC/PA (R = 0.7) with a dimension of 30 mm × 5 mm × 1 mm was heated to 180°C temperature and keep for 15 min with a static force (0.01 N). And then, an instantaneous strain of 5% was forced to the material. The stress and modulus are tested until it reaches equilibrium.

Tensile and flexural tests: the tensile and flexural properties were tested on a Universal Mechanical Testing Machine (Instron 5565A) at room temperature. For the DGEAC/PA networks, the dumbbell samples were prepared by hot pressing with a dumbbell-shaped stainless-steel mold. The sample with a dimension of 50 mm× 4 mm × 0.5 mm was tested with a gauge length of 10 mm at a crosshead speed of 2 mm/min. At least five samples were tested for all the samples. For CF/DGEAC/PA composites, the rectangle samples with a dimension of 60 mm × 15 mm × 1 mm were used for the test. A stretching speed of 2 mm/min was employed during the measurement. At least five samples were tested for all the samples.

Short beam shear test (SBS): the interlaminar shear strength (ILSS) of the sample with a dimension of 20 mm × 10 mm × 2 mm was evaluated by using the three-point short beam bending test method according to the JC 773-2010 standard. The tests were performed on a Universal Mechanical Testing Machine (Instron 5565A). The rate of crosshead motion was 1 mm/min. The ILSS value was calculated according to the equation (eq 3):

$$\mathrm{ILSS} = \frac{3P_b}{4bh} \quad \text{(eq 3)}$$

where P_b represents the maximum breaking load, b is the width of the specimen (mm), and h is the thickness of the specimen (mm).

X-ray 3D microscope imaging: the inside structure of CF/DGEAC/PA composites was investigated by using X-ray 3D microscope (nano Voxe 12000). The sample with a dimension of 10 mm × 10 mm × 1 mm was used for the tests to get images of XZ, XY, and YZ cross profile. The tests were offered by AVIC Composite Co., LTD Composite Testing Technology Center.

High-performance liquid chromatography-mass spectrometry (HPLC-MS): the HPLC analysis was carried out by an Agilent 1200 series system (Agilent Technologies 6540 Accurate-Mass Q-TOF MS). Data were acquired in positive ion mode with an ESI ion source. Sample preparation: the degradation products were placed in a 190°C oven for 12 h to evaporate EG, and then re-dissolved by adding appropriate amount of MeOH. The concentration was 5 mg/mL. Chromatographic conditions: the column is Agilent Eclipse XDB-C_{18} (4.6 × 250 mm, 5 μm); the mobile phase A was ultrapure water, B was acetonitrile, and the flow rate was 0.3 mL/min. Gradient elution conditions: 0~2 min, 5% B; 2~12 min, 5%~100% B. Conditions for electrospray mass spectrometry: dry gas temperature of 300°C, dry gas flow rate of 11 L/min, nebulizer pressure of 35 Psig, capillary voltage of 3500 V, fragmentation voltage of 125 V, mass spectrometry acquisition range of m/z 50-1000.

Raman spectra: virgin CFs and recycled CFs were measured by using an inVia-Reflex Raman spectrometer (LabRAM HR Evolution) to compare the surface chemical structures.

Scanning electronic microscopy (SEM): the morphologies of the virgin CFs, the recycled CFs, and the cleavage surface of CF/DGEAC/PA composites during the degradation process were observed using field emission scanning electron microscopy (SEM, SU8010, Japan) at an accelerating voltage of 5.0 kV. The virgin CFs and the recycled CFs need to be cleaned with acetone and dried at 50°C before observation. Meanwhile, energy dispersive spectroscopy (EDS) was performed on the virgin and the recycled CFs to investigate their chemical compositions.

3. Results and discussion

3.1 Curing and characterization of DGEAC/PA networks

The curing process of PA with DGEAC was studied by differential scanning calorimeter (DSC) with a heating rate of 5 °C /min from 50 to 250°C, where the stoichiometric ratios of DGEAC/PA (R = anhydride /epoxy group) were 0.7, 0.85, and 1.0, respectively. As shown in Fig. 1A, the narrow endothermic signal at 125°C was assigned to the melting peak of PA, and its integration increased from R = 0.7 to 1.0. Moreover, the broad exothermic peaks appeared at 150°C for R = 0.7, 0.85, and 1.0, which clearly manifested the occurrence of curing reactions. Accordingly, for covering the curing temperature range and avoiding the degradation of raw materials, the curing process was set as "130°C /1 h + 150°C /2 h + 180°C /1 h" with a pressure of 10 tons.

As shown in Fig. 1B, the cured samples of DGEAC/PA were transparent and rigid. To ensure the complete curing between PA and DGEAC, gel content and swelling ratio, two essential references for characterizing the integrity of cross-linked networks, were firstly evaluated and the results were summarized in Fig. 1C and Table S1. All networks had high gel contents (97%, 100%, and 97%) while low swelling ratios (0%, 0.7%, and 1.3%) at room temperature for R = 0.7, 0.85, and 1.0, respectively, revealing the complete cross-linked networks of DGEAC/PA. More evidences came from FTIR spectra of PA, DGEAC, and the cured DGEAC/PA. As shown in Fig. 1D, 1E and S1, the signals at 905/853 and 1740 cm^{-1} were appointed to epoxy group and ester bonds from DGEAC, while the peaks at 1854/1779 cm^{-1} were attributed to carbonyl groups from PA. After curing, both epoxy peaks from DGEAC and carbonyl groups from PA disappeared, whereas ester bonds at 1740 cm^{-1} remained and enhanced as the increase of PA content, with a generation of hydroxyl group at 3430 cm^{-1}. All these FTIR results indicated that PA and DGEAC were successfully cross-linked into the DGEAC/PA networks. In addition, no residual curing exothermic peak was

observed for DGEAC/PA networks, with only the glass transition (Fig. 1F), again demonstrating the complete curing and the amorphous nature of DGEAC/PA that was in accordance with the high transparency of cured samples. Meanwhile, the DGEAC/PA (R = 0.7) was selected to evaluate the solvent resistance. As shown in Fig. 1G, after immersing in toluene, acetone, tetrahydrofuran (THF), N, N-dimethylformamide (DMF), dimethyl sulfoxide (DMSO), MeOH, EtOH, H_2O, HCl (1 M), H_2SO_4 (1 M) and NaOH (1 M) for 96 h at room temperature, the cured DGEAC/PA remained intact, indicating that the DGEAC/PA networks not only owned good solvent resistance in organic solvents, but also in acidic and alkaline aqueous solutions.

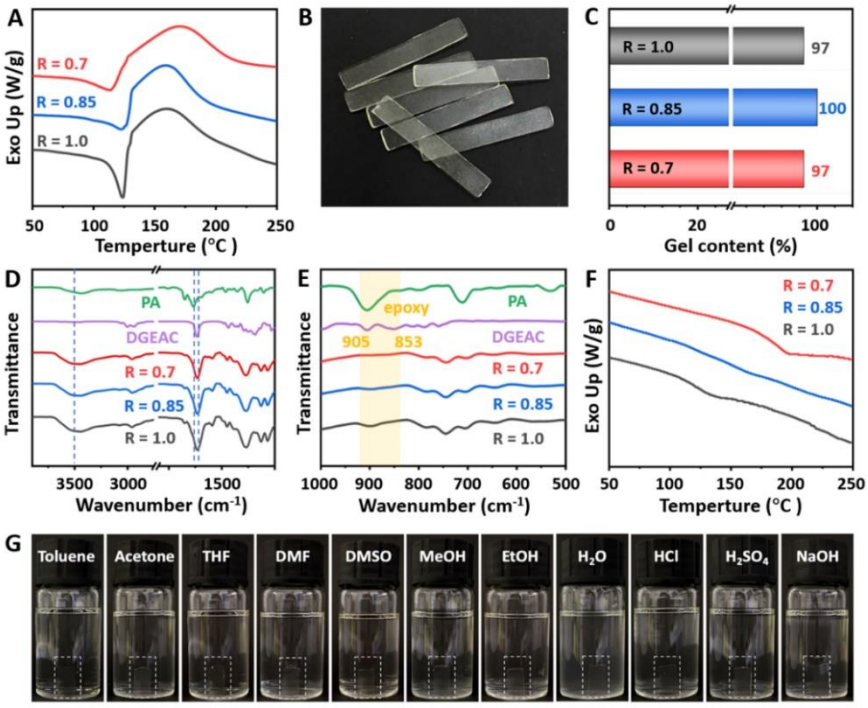

Fig. 1. (A) DSC curves of the mixture of DGEAC/PA at a heating rate of 5 °C/min. (B) Photograph of the cured DGEAC/PA samples. (C) Gel contents of DGEAC/PA networks. FTIR spectra of PA, DGEAC, and DGEAC/PA networks in the range of (D) 4000−1000

cm^{-1} and (E) 1000−500 cm^{-1}. (F) DSC curves of the cured DGEAC/PA networks at a heating rate of 5 °C/min. (G) Photographs of DGEAC/PA networks (R = 0.7) in different solvents for 96 h at room temperature. The white dotted box showed the transparent samples.

3.2 Thermal and mechanical properties of DGEAC/PA networks

The thermal stability of DGEAC/PA network was characterized by thermogravimetric analysis (TGA), where the temperature of 5% weight loss ($T_{d5\%}$) was defined as the initial degradation temperature. As shown in Fig. 2A and Table 1, the $T_{d5\%}$ of DGEAC/PA was 316, 264, and 232°C for R = 0.7, 0.85, and 1.0, respectively, implying their good thermal stability. Note that the $T_{d5\%}$ declined with the increase of PA content, because PA contained π-bonds from aromatic rings, which were less stable upon pyrolysis. For better understanding viscoelastic properties of DGEAC/PA networks, the dynamic thermomechanical analysis (DMA) was performed with a heating rate of 5 °C/min. The storage modulus curve of DGEAC/PA networks from glass to rubber plateau can be clearly seen, and the storage modulus (*G'*) of each sample (R = 0.7, 0.85, and 1.0) at the glass plateau was around 3.7 GPa. The peaks of tan δ, assigning as the glass transition temperature (T_g), were 214, 205, and 165°C for R = 0.7, 0.85, and 1.0, respectively (Fig. 2B and Table 1). It is known that T_g is usually determined by the cross-linking density and the flexibility of polymer chains [25]. Herein, the cross-linking density (v_e) of DGEAC/PA networks was calculated according to the rubber elasticity theory (eq 4):

$$v_e = E'/3RT \qquad \text{(eq 4)}$$

where *E'* is the elastic modulus in rubbery plateau region at temperature T (T_g + 40°C), T is the absolute temperature, and R is the universal gas constant (8.314 J mol^{-1} K^{-1}). The

corresponding *E'* and *ve* are concluded in Table 1. Only a slight increase in the cross-linking density was observed from R = 0.7 to 1.0. In this case, the decrease trend in T_g from R = 0.7 to 1.0 was mainly due to the polymer chains became flexible along with the involvement of more PA. Compared with R = 1.0 system, the system of R = 0.7 had more remaining hydroxyl groups after curing, which can form intermolecular hydrogen bonds, improving the rigidity of the network. It should be pointed that even the lowest T_g for R = 1.0 was still higher than that of most reported TERs-based epoxy matrices [26,27,28].

The tensile stress-strain curves of DGEAC/PA networks are presented in Fig. 2C, and the corresponding values of tensile stress, Young's modulus, and elongation at break are summarized in Fig. 2D and Table 1. Clearly, all DGEAC/PA networks exhibited excellent tensile strength, i.e. the maximum tensile strength was 79, 75, and 68 MPa for R = 0.7, 0.85, and 1.0, accompanied with the Young's modulus of 1.82, 1.84, and 1.71 GPa, respectively.

Table 1 Compositions, thermal and mechanical properties of DGEAC/PA networks

Sample[a]	$T_{d5\%}$ (°C)[b]	T_g (°C)[c]	E' (MPa)[d]	v_e (mol m^{-3})[e]	Tensile strength (MPa)[f]	Young's modulus (GPa)[f]	Elongation at break[f]
R = 0.7	316	214	81.54	6.13×10^3	79	1.82	5.5%
R = 0.85	264	205	78.43	6.14×10^3	75	1.84	4.8%
R = 1.0	232	165	74.22	6.15×10^3	68	1.71	5.3%

[a]R represents the stoichiometric ratio of anhydride/epoxy group. [b]$T_{d5\%}$ value was obtained from TGA cures in Fig. 2A. [c]T_g value was decided from the tan δ curve in Fig. 2B. [d]*E'* was obtained from storage modulus at temperature (T_g + 40°C) in Fig. 2B. [e]*ve* was calculated by

the rubber elasticity equation (eq. 4). [f]Tensile stress, Young's modulus, and elongation at break were obtained from stress-strain curves in Fig. 2C.

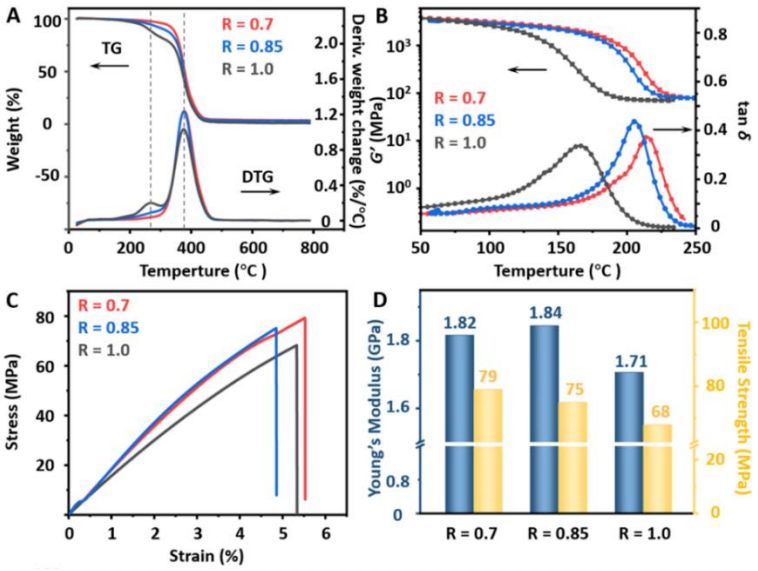

Fig. 2. (A) TGA and the corresponding DTG curves of DGEAC/PA networks at a heating rate of 10 °C/min. (B) Storage modulus (*G'*, squares) and tan δ (circle) values of DGEAC/PA networks. (C) Tensile stress-strain curves and (D) the corresponding stress and Young's modulus values of DGEAC/PA networks.

3.3 NGP effect-mediated degradation of DGEAC/PA networks

The degradability of DGEAC/PA networks (R = 0.7, 0.85, and 1.0) was performed at 190°C in ethylene glycol (EG) without extrinsic catalysts, where EG was used as the reactant and solvent. As shown in Fig. 3A, all DGEAC/PA networks degraded completely with a degradation time of 30, 36, and 39 h for R = 0.7, 0.85, and 1.0, respectively. Note that the degradation rate for R = 1.0 was faster than the one of R = 0.7 and 0.85 in the first 22 h, while slowed down after that. This was probably because more ester bonds were generated for

DGEAC/PA networks from R = 0.7 to 1.0 when curing. In this case, in the prophase of the degradation process, the existence of more ester bonds for R = 1.0 rose the probability of TERs between DGEAC/PA networks and EG molecules, thus accelerating degradation rate. In addition, the degradability kinetics of DGEAC/PA networks (R = 0.7) at different temperatures were investigated in Fig. 3B. With the increasing temperature from 190 to 195 and 200°C, the whole degradation time was shortened from 30 h to 26 h, and can be as short as 12 h, revealing the positive dependence of TERs on temperature. Apparently, this DGEAC/PA networks with excellent overall performance achieved a good degradation under auto-catalytic, alkali-free and acid-free conditions.

High performance liquid chromatography-mass spectrometry (HPLC-MS) was used to clarify the structure of the degradation products. The degraded DGEAC/PA network (R = 0.7) was selected and dissolved in MeOH to prepare the samples for HPLC-MS analysis (procedure details see ESI file). As shown in Fig. $3C_1$, there were three peaks in HPLC-MS chromatogram, corresponding to three chemicals (α, β and γ) with the retention time of 2.329, 2.593, and 2.792 min. By integrating the peak area, the content was calculated as 29.0%, 44.3%, and 26.7% for chemical α, β, and γ, respectively. Mass spectrometry cleavage features were used to determine their structures in positive ion mode with an ESI ion source. For chemical α, β, and γ, the molecular ion peak of m/z 277 $[M + Na]^+$, m/z 321 $[M + Na + H_2O]^+$ and m/z 365 $[M + K]^+$ were observed clearly (Fig. $3C_2$, C_3 and C_4), which corresponded to the molecular formula of $C_{12}H_{14}O_6$, $C_{14}H_{16}O_6$, and $C_{16}H_{22}O_7$, respectively. On the basis of these results, as well as the chemical structure of the DGEAC/PA networks (Scheme 1) and the potential reactions sites of TERs between EG and DGEAC/PA networks, the structures of chemical α, β, and γ were proposed in Fig. $3C_2$, C_3 and C_4, and their possible degradation

mechanisms were shown in Fig. S2. All these structures further confirmed the occurrence of TERs for DGEAC/PA networks.

As no extrinsic catalyst was involved in the degradation process, a neighboring group participation (NGP) effect was proposed for this TERs as illustrated in Fig. 3D. When the DGEAC/PA networks immersed in EG, the free neighboring carboxylic acid on *o*-position of benzene rings in the network preferred to form a five-membered cyclic anhydride as the transition state. This cyclic transition intermediate can act as an intrinsic nucleophilic catalyst to trigger the TERs between EG molecules and DGEAC/PA networks, consequently causing polymer chains to break into smaller segments with the end groups of hydroxyl or double bonds, and achieving complete degradation on a macroscopic scale [21,24,29]. This NPG-promoted TERs can be further confirmed by the stress relaxation experiment, where the DGEAC/PA network can quickly relax to *1/e* at 180°C without extrinsic catalysts (Fig. S3). This degradability of DGEAC/PA networks as a resin matrix will give the corresponding composites another special feature beyond the mechanical and thermal properties, which is expected to achieve non-destructive recycling of the CFs reinforcements.

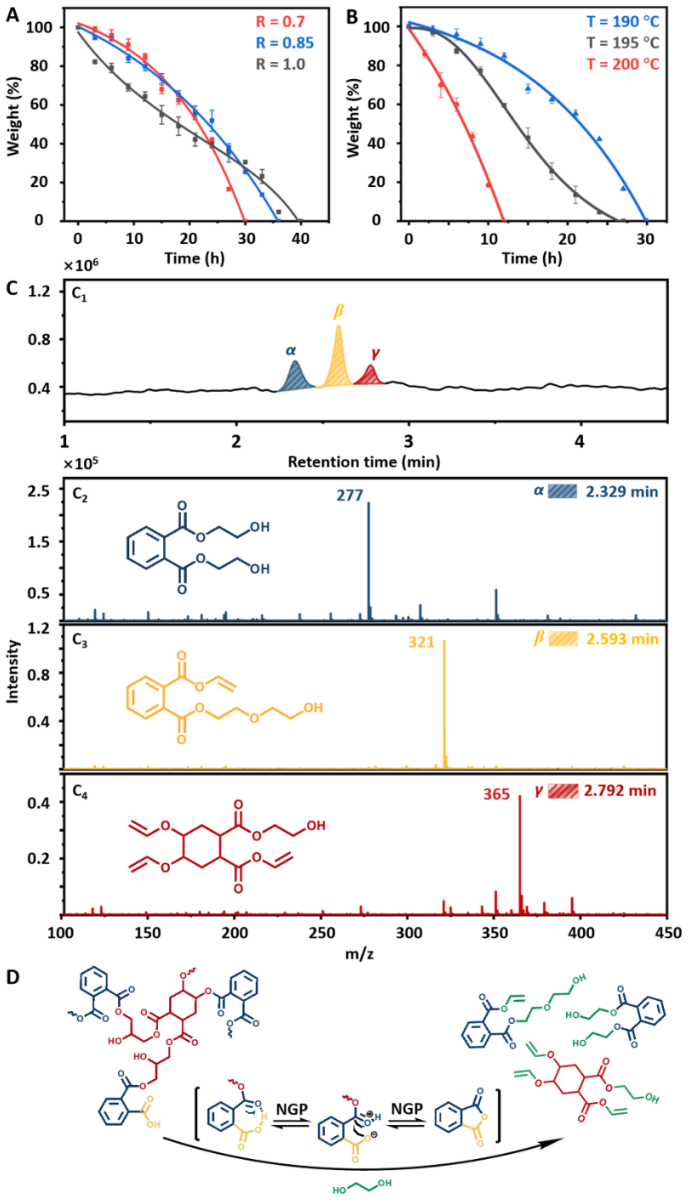

Fig. 3. (A) Degradation kinetics of DGEAC/PA networks in EG at 190°C. (B) Degradation kinetics of DGEAC/PA networks (R = 0.7) in EG at different temperatures of 190, 195, and 200°C. (C) HPLC-MS chromatogram of DGEAC/PA networks (R = 0.7). (C_1) Degradation products include α, β, and γ at the retention time of 2.328, 2.593 and 2.792 min. (C*2*) Peak α showed $[M + Na]^+$ at m/z 277, (C_3) peak β showed $[M + Na + H2O]^+$ at m/z 321, and (C_4)

peak γ showed $[M + K]^+$ at m/z 365. (D) Possible mechanism of NGP-promoted degradation of DGEAC/PA networks in EG molecules.

3.4 Preparation and characterization of CF/DGEAC/PA composites

As dictated in Scheme 1C, taking the degradable DGEAC/PA networks (R = 0.7) as matrix, the CF/DGEAC/PA composites was prepared by combining the woven T300 as reinforcement layer by layer, where the mass fraction of CFs was around 72% (Fig. 4A). The microscopic morphology of the cross-section of CF/DGEAC/PA composites was observed by scanning electron microscopy (SEM). The structure of the CFs and resin layers can be clearly seen, and the CFs tightly adhered to each other surrounded by the DGEAC/PA matrix (Fig. 4B). Moreover, the magnified image showed that the fractured surface was relatively rough due to the existence of the residual resin (inset, Fig. 4B), demonstrating the strong bonding between the DGEAC/PA matrix and the CFs. The internal structure of CF/DGEAC/PA composites was evaluated by X-ray 3D microscopy. Fig. 4C showed the whole material, while the images of YZ, XZ, and XY cross-sections were shown in Fig. 4D, 4E, and 4F, respectively. The woven structure of CFs can be clearly seen, and the absence of gaps or voids between different layers indicated that the CF/DGEAC/PA composites had the good interfacial bonding.

The mechanical properties of CF/DGEAC/PA composites were characterized via tensile-, flexural-, and short beam shear test. The tensile strength and modulus were 637 MPa and 5.02 GPa, while the flexural strength and flexural modulus were 592 MPa and 9.28 GPa, respectively (Fig. 4G and 4H). In addition, the CF/DGEAC/PA composites were used to measure the interlaminar shear strength (ILSS) for further understanding the bonding

between the matrix and the CFs. As shown in Fig. 4I and S4, the ILSS value of CF/DGEAC/PA composites was 46 MPa, higher than that of conventional CFRCs of CF/E51/DDM (E51: bisphenol-A type epoxy resin; DDM: 4,4'-diamino diphenylmethane) [30], again demonstrating the good bonding performance between the DGEAC/PA matrix and CFs.

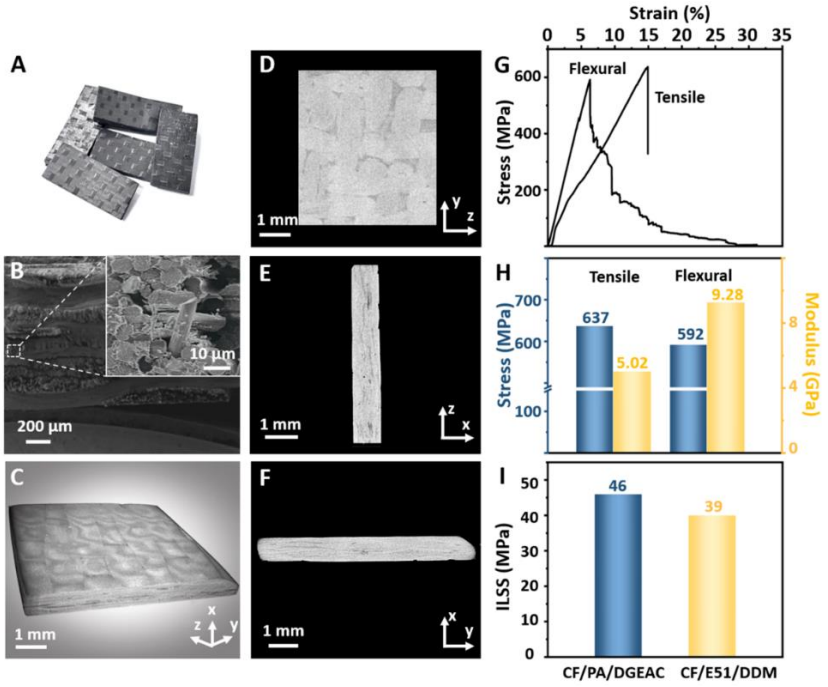

Fig. 4. (A) Photograph of the CF/DGEAC/PA composites. (B) SEM image for a cross-sectional view of the stretched CF/DGEAC/PA composites. Inset is an enlarged view of the fracture surface. X-ray 3D microscopy images of CF/DGEAC/PA composites: integral (C), YZ (D), XZ (E) and XY (F) cross profiles, respectively. Tensile and flexural stress-strain curves (G) and their corresponding stress and modulus values (H) of CF/DGEAC/PA composites. (I) ILSS values of CF/DGEAC/PA composites and the conventional CF/E51/DDM composites [30].

3.5 Recycling of CF/DGEAC/PA composites

The recovery of carbon fibers from composites without destroying their chemical structure and microscopic morphology is a common challenge. To verify whether the intact CFs could be separated and recovered for CF/DGEAC/PA composites, the degradation experiments were performed at 190°C by using EG as a reactant and solvent. The residual weight as a function of degradation time was recorded in Fig. 5A. It is obvious that the residual weight gradually decreased along with the degradation time, and reached the equilibrium after 34 h with a value of 72% that was close to the actual weight of CFs in composites, indicating that the DGEAC/PA matrix was completely degraded. In order to monitor the degradation process intuitively, the cleavage plane of CF/DGEAC/PA composites was observed by SEM images at different degradation time. As shown in Fig. 5D, the cleavage surface of CF/DGEAC/PA composites owned a robust interface between the matrix and CFs before degradation, which agreed well with the X-ray 3D microscopy in Fig. 4B and 4C. After 15 h, a small portion of the matrices degraded, and some CFs were exposed. Up to 21 h, a large number of matrices were lessened, which permitted sleek fiber bundles to be found. Lastly, nearly all the matrices were removed from the CFs after 34 h, and the surface of CFs became remarkable smooth.

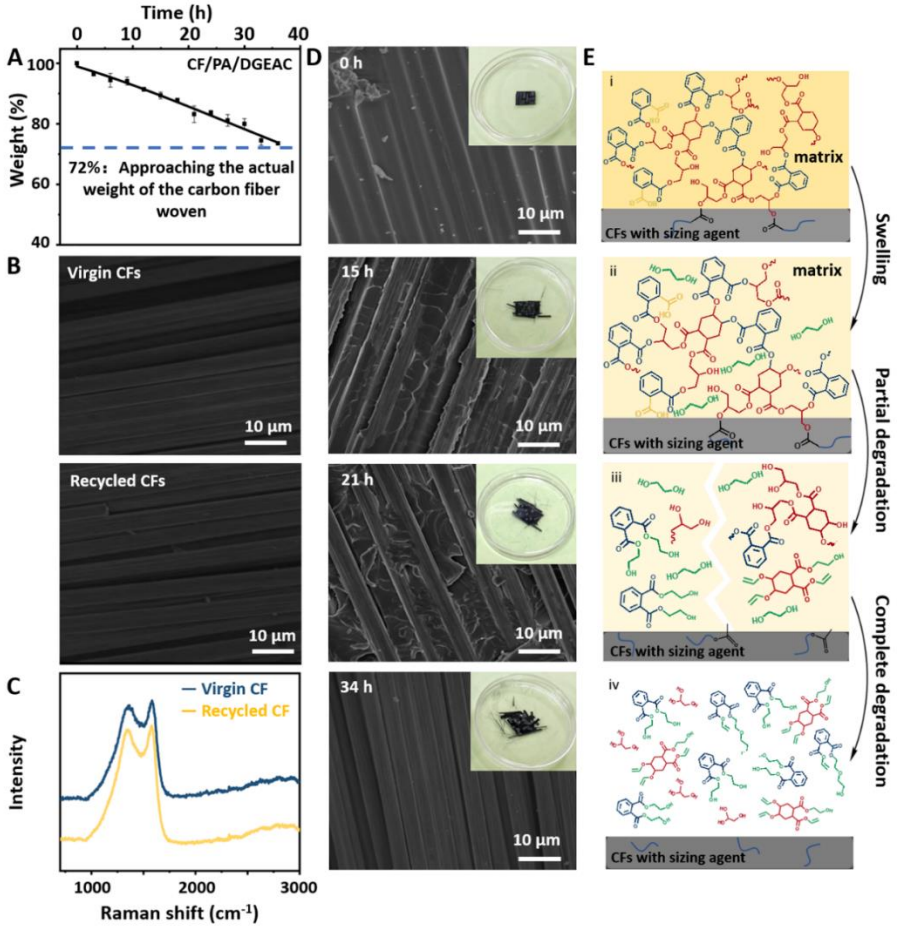

Fig. 5. (A) Degradation kinetics of CF/DGEAC/PA composites in EG at 190°C. (B) SEM images of the surface morphology of the virgin and recycled CFs. (C) Raman spectra of the virgin and recycled CFs. (D) SEM images of the cleavage plane of CF/DGEAC/PA composites at the degradation time of 0, 15, 21, and 34 h. The top right corner shows the photo of composites at the corresponding degradation time. (E) Possible degradation mechanism of CF/DGEAC/PA composites in EG at 190°C. (i) DGEAC/PA matrix was swollen in EG at 190°C; (ii) DGEAC/PA matrix was involved in TERs at 190°C; (iii) DGEAC/PA matrix was partially degraded by EG; (iv) DGEAC/PA matrix was completely degraded in EG at 190°C.

Fig. 5B showed that the microstructure of the recycled CFs was clean and smooth, similar to that of the virgin CFs, demonstrating again that the DGEAC/PA matrix was completely degraded. In addition, the chemical structures of the virgin and the recycled CFs were analyzed by Raman spectra in Fig. 5C, where no difference was observed, indicating that the degradation hardly affected the graphitized structure of CFs. More evidences came from SEM-energy dispersive spectroscopy (EDS), in which the chemical compositions of the virgin CFs and the recycled CFs were almost the same (Fig. S5). On the basis of the above results, as well as the degradation mechanism of pure DGEAC/PA matrix, the degradation process of CF/DGEAC/PA composites was proposed in Fig. 5E. Initially, the DGEAC/PA matrix was swollen, allowing EG molecules to access the polymer networks. After that, promoted by the neighboring group participation (NGP) effect, the hydroxyl group of EG molecules participated in the TERs at 190°C, leading to the partial degradation of the cross-linked DGEAC/PA network. Along with the degradation time, all the ester bonds in the network were degraded, affording the clean recycled CFs. Collectively, the CF/DGEAC/PA composites exhibited the comprehensive performance in comparison with the reported degradable composites containing dynamic covalent cross-linked networks (Table S2). On one hand, the CF/DGEAC/PA composites were prepared from the commercial-scale raw materials at low price, showing good solvent resistance and thermal/mechanical properties comparable to conventional and dynamically cross-linked resin-based composites. On the other hand, under the auto-catalytic condition the composites could be degraded with a moderate time and the CFs would be recycled with the similar features of the virgin ones.

4. Conclusions

By using commercial-scale low-cost phthalic anhydride (PA) and diglycidyl ester of aliphatic cyclo (DGEAC) as raw materials, the dynamic ester bonds-containing DGEAC/PA networks with different stoichiometric ratios of anhydride/epoxy groups were prepared through an auto-catalytic curing process. This DGEAC/PA networks not only exhibited good resistance to common organic solvents, acidic and alkaline aqueous solutions, but also had excellent thermal stability with a T_g ranging from 165 to 214°C, mechanical strength from 68 to 79 MPa, and Young's modulus from 1.71 to 1.82 GPa. More importantly, the neighboring free carboxylic acid on *o*-position of benzene rings in the networks preferred to form a five-membered cyclic transition state during the TERs process, which can act as an intrinsic nucleophilic catalyst to trigger the TERs without the help of extrinsic catalyst. Benefiting from this neighboring group participation (NGP) effect, the DGEAC/PA network can achieve complete degradation in ethylene glycol. Taking this degradable DGEAC/PA network (R = 0.7) as the matrix, the CF/DGEAC/PA composites were further fabricated by combining the CFs layer by layer. The CF/DGEAC/PA composites showed the tensile strength and modulus of 637 MPa and 5.02 GPa, while the flexural strength and flexural modulus of 592 MPa and 9.28 GPa. In addition, its interlaminar shear strength was around 46 MPa, comparable to that of conventional epoxy composites like CF/E51/DDM. Meanwhile, because of the degradability of the DGEAC/PA matrix, the intact CFs can be recycled with characteristics similar to those of virgin CFs. This work provides a simple yet green strategy to prepare high-performance and recyclable CFRCs, which is promising for industrial application.

Declaration of competing interest

The authors declare that they have no known competing financial interests or personal relationships that could have appeared to influence the work reported in this paper.

Acknowledgements

This work is supported by the Open Fund of National Key Laboratory of Science and Technology on Advanced Composite (KZ42191814).

Appendix A. Supplementary data

Supplementary data to this article can be found online.

References

[1] Jin FL, Li X, Park SJ. Synthesis and application of epoxy resins: A review. J. Ind. Eng. Chem. 2015; 29: 1-11, https://doi.org/10.1016/j.jiec.2015.03.026.

[2] Oliveux G, Dandy LO, Leeke GA. Current status of recycling of fibre reinforced polymers: review of technologies, reuse and resulting properties. Prog. Mater. Sci. 2015; 72: 61-99, https://doi.org/10.1016/j.pmatsci.2015.01.004.

[3] Mativenga PT, Shuaib NA, Howarth J, Pestalozzi F, Woidasky J. High voltage fragmentation and mechanical recycling of glass fibre thermoset composite. Cirp Ann-Manuf Techn. 2016; 65: 45-48, https://doi.org/10.1016/j.cirp.2016.04.107.

[4] Navarro CA, Giffin CR, Zhang B, Yu Z, Nutt SR, Williams TJ. High voltage fragmentation and mechanical recycling of glass fibre thermoset composite. Mater. Horiz. 2020; 7: 2479-2486, https://doi.org/10.1039/D0MH01085E.

[5] Palmer J, Ghita OR, Savage L, Evans KE. Compos. Successful closed-loop recycling of thermoset composites. Part A-Appl. S. 2009; 40: 490-498, https://doi.org/10.1016/j.compositesa.2009.02.002.

[6] Knappich F, Klotz M, Schlummer M, Wolling J, Maurer A. Recycling process for carbon fiber reinforced plastics with polyamide 6, polyurethane and epoxy matrix by gentle solvent treatment. Waste Manage. 2019; 85: 73-81, https://doi.org/10.1016/j.wasman.2018.12.016.

[7] Jiang JJ, Deng GL, Chen X, Gao XY, Guo Q, Xu CM, et al. On the successful chemical recycling of carbon fiber/epoxy resin composites under the mild condition. Compos. Sci. Technol. 2017; 151: 243-251, https://doi.org/10.1016/j.compscitech.2017.08.007.

[8] Ma SQ, Wei JJ, Jia Z, Yu T, Yuan WC, Zhu J, et al. Readily recyclable, high-performance thermosetting materials based on a lignin-derived spiro diacetal trigger. J. Mater. Chem. A 2019; 7: 1233-1243, https://doi.org/10.1039/C8TA07140C.

[9] Wang S, Ma SQ, Li Q, Xu XW, Wang BB, Yuan WC, et al. Facile in situ preparation of high-performance epoxy vitrimer from renewable resources and its application in nondestructive recyclable carbon fiber composite. Green Chem. 2019; 21: 1484-1497, https://doi.org/10.1039/C8GC03477J.

[10] Liu YY, Liu GL, Li YD, Weng YX, Zeng JB. Biobased high-performance epoxy vitrimer with UV shielding for recyclable carbon fiber reinforced composites. ACS Sustain. Chem. Eng. 2021; 9: 4638-4647, https://doi.org/10.1021/acssuschemeng.1c00231.

[11] Memon H, Wei Y, Zhang LY, Jiang QR, Liu WS. An imine-containing epoxy vitrimer with versatile recyclability and its application in fully recyclable carbon

fiber reinforced composites. Compos. Sci. Technol. 2020; 199: 108314, https://doi.org/10.1016/J.COMPSCITECH.2020.108314.

[12] Yu K, Shi Q, Dunn ML, Wang TJ, Jerry QH. Carbon fiber reinforced thermoset composite with near 100% recyclability. Adv. Funct. Mater. 2016; 26: 6098-6106, https://doi.org/10.1002/adfm.201602056.

[13] Liu YL, Wang BB, Ma SQ, Yu T, Xu XW, Li Q, et al. Catalyst-free malleable, degradable, bio-based epoxy thermosets and its application in recyclable carbon fiber composites. Compos. Part B-Eng. 2021; 211: 108654, https://doi.org/10.1016/J.COMPOSITESB.2021.108654.

[14] Liu T, Hao C, Shao L, Kuang W, Cosimbescu L, Zhang JW, et al. Carbon fiber reinforced epoxy vitrimer: robust mechanical performance and facile hydrothermal decomposition in pure water. Macromol. Rapid Commun. 2021; 42: 2000458, https://doi.org/10.1002/MARC.202000458.

[15] Luzuriaga ARD, Martin R, Markaide N, Rekondo A, Odriozola I. Epoxy resin with exchangeable disulfide crosslinks to obtain reprocessable, repairable and recyclable fiber-reinforced thermoset composites. Mater. Horiz. 2016; 3: 241-247, https://doi.org/10.1039/C8TA07140C.

[16] Si HW, Zhou L, Wu YP, Song LX, Kang M, Chen M, et al. Rapidly reprocessable, degradable epoxy vitrimer and recyclable carbon fiber reinforced thermoset composites relied on high contents of exchangeable aromatic disulfide crosslinks. Compos. Part B-Eng. 2020; 199: 108278, https://doi.org/10.1016/J.COMPOSITESB.2020.108278.

[17] Montarnal D, Capelot M, Tournilhac F, Leibler L, Silica-like malleable materials from permanent organic networks. Science 2011; 334: 965-968, https://doi.org/10.1126/science.1212648.

[18] Liu T, Zhao BM, Zhang JW. Recent development of repairable, malleable and recyclable thermosetting polymers through dynamic transesterification. Polymer 2020; 194: 122392, https://doi.org/10.1016/J.POLYMER.2020.122392.

[19] Han JR, Liu T, Hao C, Zhang S, Guo BH, Zhang JW. A Catalyst-free epoxy vitrimer system based on multifunctional hyperbranched polymer. Macromolecules 2018; 51: 6789-6799, https://doi.org/10.1021/acs.macromol.8b01424.

[20] Liu T, Zhang S, Hao C, Verdi C, Liu W, Zhang JW, et al. Glycerol induced catalyst-free curing of epoxy and vitrimer preparation. Macromol. Rapid Commun. 2019; 40: e1800889, https://doi.org/10.1002/marc.201800889.

[21] Delahaye M, Winne JM, Du Prez FE. Internal catalysis in covalent adaptable networks: phthalate monoester transesterification as a versatile dynamic cross-linking chemistry. J. Am. Chem. Soc. 2019; 141: 15277-15287, https://doi.org/10.1021/jacs.9b07269.

[22] Podgorski M, Mavila S, Huang S, Spurgin N, Sinha J, Bowman CN. Thiol-anhydride dynamic reversible networks. Angew. Chem. Int. Ed. 2020; 59: 9345-9349, https://doi.org/10.1002/ANIE.202001388.

[23] Zhang HY, Majumdar S, van Benthem RATM, Sijbesma RP, Heuts JPA. Intramolecularly catalyzed dynamic polyester networks using neighboring carboxylic and sulfonic acid groups. ACS Macro. Lett. 2020; 9: 272-277, https://dx.doi.org/10.1021/acsmacrolett.9b01023.

[24] Delahaye M, Tanini F, Holloway JO, Winne JM, Du Prez FE. Double neighbouring group participation for ultrafast exchange in phthalate monoester networks. Polym. Chem. 2020; 11: 5207-5215, https://doi.org/10.1039/D0PY00681E.

[25] Yang XX, Guo LZ, Xu X, Shang SB, Liu H. A fully bio-based epoxy vitrimer: Self-healing, triple-shape memory and reprocessing triggered by dynamic covalent bond exchange. Mater. Design 2020; 186: 108248, https://doi.org/10.1016/j.matdes.2019.108248.

[26] Altuna FI, Pettarin V, Williams RJJ, Self-healable polymer networks based on the cross-linking of epoxidised soybean oil by an aqueous citric acid solution. Green Chem. 2013; 15: 3360-3366, https://doi.org/10.1039/C3GC41384E.

[27] Cunha RH, Nele M, Dias ML. Reaction and thermal behavior of vitrimer-like polyhydroxy esters based on polyethylene glycol diglycidyl ether. J. Appl. Polym. Sci. 2020; 137: 49329, https://doi.org/10.1002/app.49329.

[28] Altuna FI, Hoppe CE, Williams RJJ. Epoxy vitrimers with a covalently bonded tertiary amine as catalyst of the transesterification reaction. Eur. Polym. J. 2019; 113: 297-304, https://doi.org/10.1016/j.eurpolymj.2019.01.045.

[29] Van Lijsebetten F, Holloway JO, Winne JM, Du Prez FE. Internal catalysis for dynamic covalent chemistry applications and polymer science. Chem. Soc. Rev. 2020; 49: 8425-8438, https://doi.org/10.1039/D0CS00452A.

[30] Qiu BW, Sun T, Li MX, Chen Y, Zhou ST, Liang M, et al. High micromechanical interlocking graphene oxide/carboxymethyl cellulose composite architectures for

enhancing the interface adhesion between carbon fiber and epoxy. Compos. Part A Appl. S. 2020; 139: 106092, https://doi.org/10.1016/j.compositesa.2020.106092.